

Unbalanced droplets of one-dimensional mixtures of fermions

M. C. Gordillo^{1,2,*}

¹*Departamento de Sistemas Físicos, Químicos y Naturales,
Universidad Pablo de Olavide, Carretera de Utrera km 1, E-41013 Sevilla, Spain*

²*Instituto Carlos I de Física Teórica y Computacional,
Universidad de Granada, E-18071 Granada, Spain.*

(Dated: October 3, 2024)

By means of a diffusion Monte Carlo technique, we study one-dimensional mixtures of fermionic Ytterbium atoms (^{173}Yb , ^{171}Yb) in which the total number of ^{173}Yb particles is different from the sum of all the atoms belonging to the ^{171}Yb isotope. Even though self-bound droplets are possible for different compositions, the most stable ones are clusters with a slight excess of attractively interacting ^{171}Yb particles belonging to different spins with respect to the number of spin-polarized ^{173}Yb atoms.

I. INTRODUCTION

A droplet can be defined as a (relatively) small cluster of particles that stick together without collapse or evaporation during a reasonable long period of time. To be considered self-bound, a droplet has to be stable without the intervention of an external confining potential. When several species are present, the outcome of the mixing would depend on factors as the bosonic or fermionic nature of the particles, their repulsive or attractive interactions and the dimensionality of the system [1–3]. The seminal work by Petrov [4], opened the field for ultracold Bose-Bose droplets [1, 2, 5–13], but Bose-Fermi [14–18] and Fermi systems [19–21] are also viable alternatives.

Within this context, the consideration of one-dimensional (1D) systems offers the advantage of the suppression of three-body losses with respect to their three-dimensional counterparts [3, 22]. In addition, if the interactions between species are the right ones, we can have self-bound Bose-Bose [11–13], Bose-Fermi [14, 17], and Fermi-Fermi 1D droplets [19, 20]. This last case is a bit problematic, specially when we consider species interacting via strictly 1D short-range interactions. Under such circumstances, to have a stable droplet we need at least two kinds of particles with attractive interactions between them, typically atoms belonging to the same isotope but with different spins. Unfortunately, when the number of spin-ups equals the number of spin-downs, we end up with a set of composite bosons (or "molecules") with an effective repulsion between them [23, 24] that makes self-bound balanced 1D clusters of fermions impossible [19, 25].

Fortunately, there is a way to circumvent that limitation: to consider at least three different types of fermionic species [19, 20]. This has been proved to work in small clusters of Ytterbium (^{173}Yb and ^{171}Yb) with attractive interactions between atoms belonging to different isotopes. In droplets with the same number of ^{173}Yb and ^{171}Yb atoms, the mechanism to make those Fermi-Fermi

arrangements stable comes from realizing that atoms belonging to the same isotope can have different spins. In that way, not all the ^{173}Yb - ^{171}Yb molecules are equal: we have as many types of composite bosons as possible spin pairings. Then, the relaxation of the Pauli avoidance between different kinds of molecules allows the attractive interaction between them to kick in, producing self-bound droplets.

In this work, we will continue to deal with those alkali-earth atom-like mixtures, but removing the constriction of having the same number of atoms belonging to the ^{173}Yb and ^{171}Yb isotopes (N_{173} and N_{171} , respectively). We will check whether it is possible to have self-bound unbalanced 1D clusters, i.e., arrangements with $N_{173} \neq N_{171}$. To simplify things, we will consider only situations in which one of the components (either ^{173}Yb and ^{171}Yb) is spin-polarized while the atoms of the other are equally split into two sets that have different spins.

II. METHOD

Following the previous literature, the 1D clusters in this work will be described by the following Hamiltonian [19, 20, 26, 27]:

$$\begin{aligned} H = & \sum_{i=1}^{N_p} \frac{-\hbar^2}{2m} \nabla_i^2 + g_{1D}^{173-171} \sum_{i=1}^{N_{173}} \sum_{j=1}^{N_{171}} \delta(x_i^{173} - x_j^{171}) \\ & + g_{1D}^{173-173} \sum_{b>a} \sum_{i=1}^{n_{173,a}} \sum_{j=1}^{n_{173,b}} \delta(x_{a,i}^{173} - x_{b,j}^{173}) \\ & + g_{1D}^{171-171} \sum_{b>a} \sum_{i=1}^{n_{171,a}} \sum_{j=1}^{n_{171,b}} \delta(x_{a,i}^{171} - x_{b,j}^{171}), \quad (1) \end{aligned}$$

where N_p is the total number of fermions, with $N_p = N_{173} + N_{171}$, and will be in the range 24–36. As indicated above, $N_{173} \neq N_{171}$. Eq. 1 considers only interactions in which the atoms in the pair are different from each other, since Pauli's exclusion principle takes care of the avoidance between identical fermions. m is the mass of the atoms, described by a single parameter as in the previous literature [19, 20, 26, 27]. $n_{173,ab}$ and $n_{171,ab}$ are

* cgorbar@upo.es

the number of atoms with spins a and b . The g_{1D} parameters depend on the 1D-scattering lengths, a_{1D} , via $g_{1D}^{\alpha,\beta} = -2\hbar^2/ma_{1D}(\alpha,\beta)$, with a_{1D} defined by [28]:

$$a_{1D}(\alpha,\beta) = -\frac{\sigma_{\perp}^2}{a_{3D}(\alpha,\beta)} \left(1 - A \frac{a_{3D}(\alpha,\beta)}{\sigma_{\perp}} \right), \quad (2)$$

with $A=1.0326$ and $(\alpha,\beta) = (173,171)$. $\sigma_{\perp} = \sqrt{\hbar/m\omega_{\perp}}$ is the oscillator length in the transverse direction, depending on the perpendicular confinement frequency, ω_{\perp} , taken to be in the range $2\pi \times 50\text{-}100$ kHz, tight enough to produce a quasi-one dimensional system. $a_{3D}(\alpha,\beta)$ are the three-dimensional experimental scattering lengths between isotopes, taken from Ref. 29. Since no confining-induced resonance is possible in the considered range of frequencies, the nature of the interactions between isotopes is fixed by the sign of those a_{3D} 's: attractive for the $^{173}\text{Yb-}^{171}\text{Yb}$ and $^{171}\text{Yb-}^{171}\text{Yb}$ pairs and repulsive in the $^{173}\text{Yb-}^{173}\text{Yb}$ case.

To solve the Schrödinger equation derived from the Hamiltonian in Eq. 1, we used the fixed-node diffusion Monte Carlo (FN-DMC) algorithm, that gives us the exact ground state of a 1D system of fermions [30, 31] starting from an initial approximation to the exact wavefunction, the so-called trial function. We used:

$$\begin{aligned} \Phi(x_1, \dots, x_{N_p}) = & \\ \mathcal{A}(x_1^{173}, x_2^{173}, \dots, x_{N_{173}}^{173}, x_1^{171}, x_2^{171}, \dots, x_{N_{171}}^{171}) & \\ \prod_{b>a} \prod_{i=1}^{n_{173,a}} \prod_{j=1}^{n_{173,b}} \frac{\psi(x_{a,i}^{173} - x_{b,j}^{173})}{(x_{a,i}^{173} - x_{b,j}^{173})} & \\ \prod_{b>a} \prod_{i=1}^{n_{171,a}} \prod_{j=1}^{n_{171,b}} \frac{\psi(x_{a,i}^{171} - x_{b,j}^{171})}{(x_{a,i}^{171} - x_{b,j}^{171})}, & \quad (3) \end{aligned}$$

where $\mathcal{A}(x_1^{173}, x_2^{173}, \dots, x_{N_{173}}^{173}, x_1^{171}, x_2^{171}, \dots, x_{N_{171}}^{171})$ is the determinant of a square matrix that depends on the coordinates all the particles in the system. The dimension of that square matrix will be $N_{max} \times N_{max}$, N_{max} being the maximum value between N_{173} and N_{171} . To build that matrix, we followed the prescription used in Ref. 32 for unbalanced sets of fermions. If, for the sake of the argument, we consider $N_{max} = N_{171} > N_{173}$, we will have a $N_{171} \times N_{171}$ matrix. Bearing in mind that the solutions of the Schrödinger equation for a pair of 1D-particles interacting via an attractive delta potential can be written as [33]:

$$\phi(|x_i^{173} - x_j^{171}|) = \exp \left[-\frac{|g_{1D}^{173,171}|}{2} |x_i^{173} - x_j^{171}| \right], \quad (4)$$

then, we have that the first N_{173} rows of that $N_{171} \times N_{171}$ matrix are of the form:

$$\phi(|x_i^{173} - x_1^{171}|), \phi(|x_i^{173} - x_2^{171}|), \dots, \phi(|x_i^{173} - x_{N_{171}}^{171}|), \quad (5)$$

with i in the range $i=1, \dots, N_{173}$. The remaining $N_{171} - N_{173}$ rows have to include functions that depend exclusively on the coordinates of all the atoms of the ^{171}Yb

isotope. Following Ref. 34, we considered single-particle orbitals similar to the ones we would have in a Vandermonde matrix [35]. This means that the complete $N_{171} \times N_{171}$ determinant can be written as:

$$\begin{vmatrix} x_{1'}^{N_{171}-N_{173}-1} & x_{2'}^{N_{171}-N_{173}-1} & \dots & x_{N_{171}}^{N_{171}-N_{173}-1} \\ \dots & \dots & \dots & \dots \\ x_{1'}^2 & x_{2'}^2 & \dots & x_{N_{171}}^2 \\ x_{1'} & x_{2'} & \dots & x_{N_{171}} \\ 1 & 1 & \dots & 1 \\ \phi(r_{N_{173},1'}) & \phi(r_{N_{173},2'}) & \dots & \phi(r_{N_{173},N_{171}}) \\ \dots & \dots & \dots & \dots \\ \phi(r_{2,1'}) & \phi(r_{2,2'}) & \dots & \phi(r_{2,N_{171}}) \\ \phi(r_{1,1'}) & \phi(r_{1,2'}) & \dots & \phi(r_{1,N_{171}}) \end{vmatrix}$$

with $r_{i,j'} = |x_i^{173} - x_{j'}^{171}|$. This form does not include any confining wavefunction, as it is typically the case when an harmonic potential is included in the Hamiltonian [35].

The terms $(x_{a,i}^{\alpha} - x_{b,j}^{\alpha})$ in the denominator of Eq. 3 correct the spurious nodes between atoms of the same isotope with different spins (see Refs. 19 and 26 for further details). In Eq. 3, $\psi(x_{a,i}^{\alpha} - x_{b,j}^{\alpha})$'s are Jastrow functions that introduce the correlations between pairs of particles of the same isotope belonging to different spin species a, b . For the repulsively interacting $^{173}\text{Yb-}^{173}\text{Yb}$ pair, we have [36]:

$$\psi(x_{a,i}^{173} - x_{b,j}^{173}) = \cos(k[|x_{a,i}^{173} - x_{b,j}^{173}| - R_m]) \quad (6)$$

when the distance between atoms, $|x_{a,i}^{173} - x_{b,j}^{173}|$, was smaller than a variationally obtained parameter, R_m , and 1 otherwise. k was obtained by solving the transcendental equation $ka_{1D}(173,173) \tan(kR_m) = 1$. When the pair of particles of the same isotope attract each other, as in the $^{171}\text{Yb-}^{171}\text{Yb}$ case, the Jastrow has the form of Eq. 4 [26, 36], but with a different value of the defining constant, $g_{1D}^{171,171}$.

III. RESULTS

As shown in previous literature [19, 25], when $N_{173}=N_{171}$ and the atoms belonging to both isotopes are spin-polarized, we have a set of composite bosons with an effective repulsion between them due to a double Pauli avoidance that precludes the formation of self-bound clusters. One of the tell-tale signals of this behavior is that the energy per particle is exactly $E_b/2 = -(g_{1D}^{173,171})^2/(8\hbar\omega_{\perp}\sigma_{\perp})$, with E_b the binding energy of a pair of particles interacting attractively via a 1D delta potential [33]. On the other hand, when $N_{171} > N_{173}$ (again for the sake of the argument) what we have is that the total energy of the system is $N_{173}E_b$. In Figs. 1-3 and Fig. 5, we display the dependence of the energy per particle on the cluster composition to check whether is smaller than $(N_{173}/N_p)E_b$ (or $(N_{171}/N_p)E_b$, depending on the case) and self-bound droplets are possible.

The first of those figures show the case for clusters with total number of particles in the range 24-30, assembled

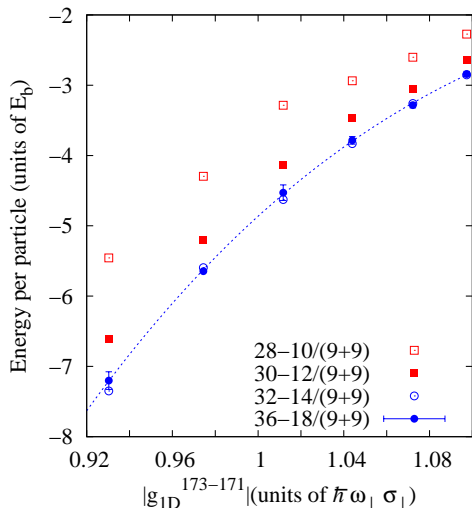


FIG. 1. Energies per Yb atom for clusters of different compositions (see text for definitions) as a function of the interaction parameter between atoms of different isotopes. Error bars in all cases are similar to the ones displayed and not shown for simplicity. Dotted line is a least-squares third order polynomial fit to the 36-18/(9+9) case and it is intended as a guide-to-the-eye.

by joining together a variable number of spin-polarized ^{173}Yb atoms and a evenly distributed set of spin-up and spin-down ^{171}Yb particles. In this example, we fixed $N_{171}/2 = 9$, but the results are similar for clusters with different compositions. To name those clusters, we used the convention $N_p - N_{173} / (N_{171}/2 + N_{171}/2)$. Since their energies per particle are smaller than E_b , we may say that, in principle, the droplets are self-bound, this being due to the attractive interactions between atoms in different (with unequal spins for the atoms in the ^{171}Yb isotope) molecules. We can see also that, for the same total number of ^{171}Yb atoms, the stability of the cluster increases with the number of ^{173}Yb particles.

On the other hand, when we keep N_{173} constant, the energy per particle also decreases with N_{171} , as can be seen in Fig. 2. However, one may wonder how those trends balance for clusters with a fixed number of particles. To answer that, we display in Fig. 3, a couple of representative examples that indicate that, when N_p is constant the most stable arrangements are those with a small imbalance in the N_{173}/N_{171} ratio.

However, to make sure that we have a stable self-bound droplet we have to check that the cluster will not eventually break during the course of the simulation. To do that, we calculated the density profiles for different arrangements and checked that they remained invariant and finite in width throughout each simulation. As a example of such circumstance, we display in Fig. 4 one of those profiles for a 28-12/(8+8) droplet, representative of clusters in which the spin-polarized component is ^{173}Yb ,

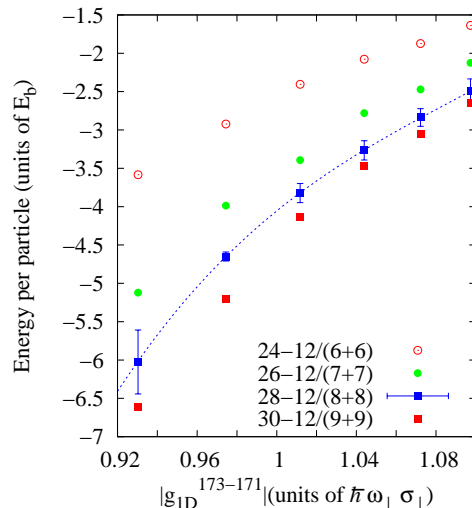


FIG. 2. Same as in Fig. 1 but for clusters in which the number of atoms in the spin-polarized ^{173}Yb subcluster is fixed. As in the previous figure, the error bars are comparable in all cases and only shown for the 28-12/(8+8) droplet for clarity. The dotted line is also intended as a guide-to-the-eye.

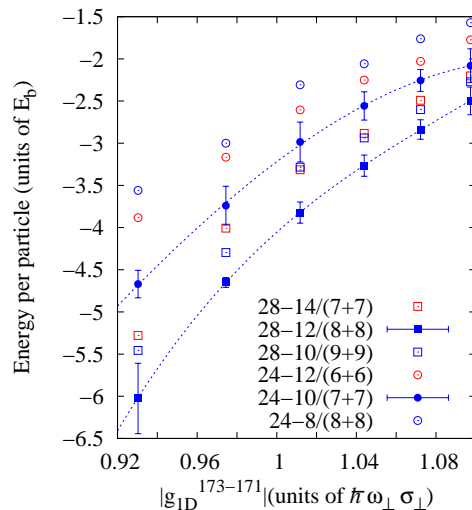


FIG. 3. Energies per particle for different cluster compositions. In all cases the error bars are of the size of the ones displayed and the dotted lines are again guides-to-the-eye.

for two different values of transverse confinement. The profiles are normalized to the total number of particles for the ^{173}Yb isotope (12) and to the number of particles per spin for the ^{171}Yb one (8). Those are equilibrium profiles, unchanged along a DMC simulation comprising 3×10^5 Monte Carlo steps after thermalization and averaged over 3 independent Monte Carlo histories. To avoid spurious correlations, we considered only configurations

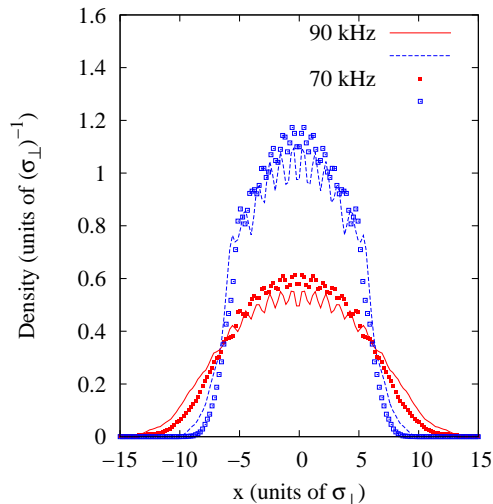


FIG. 4. Density profiles for a 28-12/(8+8) cluster for two different values of transverse confinement. Open symbols and dashed line correspond to ^{173}Yb densities, while solid symbols and full line display the behavior of each spin component of the ^{171}Yb isotope. Error bars are of the size of the symbols and not displayed by simplicity.

separated 100 steps apart, i.e., we kept 3000 sets of data. To be sure about stability of the clusters, we compared those total averages with the ones obtained considering the first 1000 DMC steps, the 1000 in the middle, and the 1000 final configurations of each history. In all cases, the results were identical to those shown in Fig. 4. As to the properties of the droplet itself, we can see that the tighter the confinement, the larger the spread of the atoms of the cluster in the longitudinal direction, in accordance with what happens in balanced clusters [19]. We can see also that the ^{171}Yb densities spread outside the locations of the spin-polarized ^{173}Yb isotope, but not too far. This allows the excess ^{171}Yb atoms in the wings to bind with the ^{173}Yb 's closer to them.

Fig. 5 gives us the same information as Fig. 1, but for arrangements in which the spin-polarized component belongs to the ^{171}Yb isotope. This implies that the interactions between the two sets of ^{173}Yb atoms are repulsive, as corresponds to the positive three-dimensional scattering length [29] between them. In that figure, we only display energies per particle for two clusters. The reason is that they are the only two for which the density profiles are stable according to the criterion described in the previous paragraph. When the number of ^{171}Yb decreases (or, equivalently, the number of ^{173}Yb increases), the clusters end up either splitting into smaller units or regularly spreading along the simulation runs with no equilibrium final position. This last circumstance would be akin to "evaporation". The density profile for the stable 35-(9+9)/17 cluster is displayed in Fig. 6. There, we can see that this droplet is wider than its counterpart

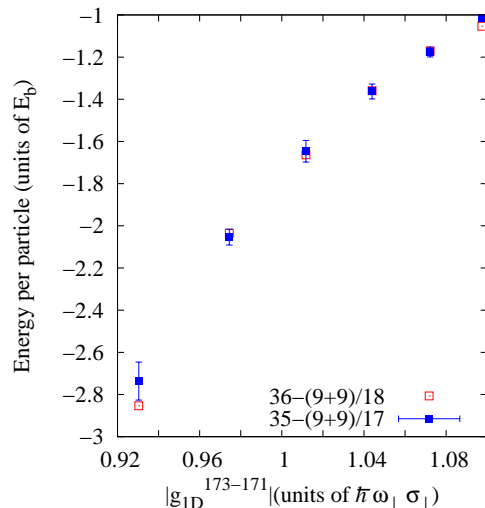


FIG. 5. Energies per particle for stable clusters in which the spin-polarized component is ^{171}Yb . Error bars are similar in both cases, but they are only shown for the 35-(9+9)/17 cluster.

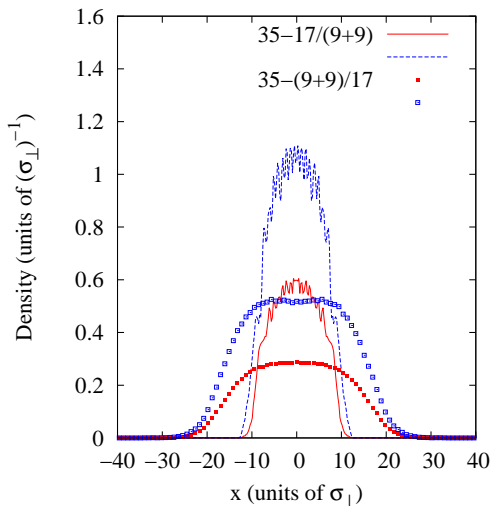


FIG. 6. Same as in Fig. 4 for two different droplets with the same size and different compositions for a transverse confinement of $\omega_{\perp} = 2\pi \times 90$ Hz. Dashed lines and open symbols correspond to the spin-polarized component, while solid lines and symbols show the results for one of the spin components corresponding to atoms in the other isotope.

of the same size. Obviously, this is due to the repulsive interactions between atoms in the (9+9) subcluster. In any case, the nine atom subunits are contained within the limits of their spin-polarized counterparts and the whole cluster is stable due to the attractive ^{171}Yb - ^{173}Yb interactions.

IV. CONCLUSIONS

In this work we have dealt with the possibility of having 1D self-bound unbalanced clusters of fermions. By that, we meant mixtures of Ytterbium isotopes in which the total number of ^{173}Yb atoms is different than the total number of ^{171}Yb particles. As in the case of balanced droplets ($N_{173}=N_{171}$), when both components are spin-polarized, it is impossible to have a self-bound system. On the other hand, when the atoms of one of the isotopes have different spin values, those droplets are stable. In this work we have considered only examples of evenly split spin populations, but the results are similar for other distributions.

We saw also that the relative stability of the droplets depends on their composition. Unbalanced droplets in which the interactions between particles of the same isotope and unequal spins are repulsive have a very narrow stability range. What we have found is that when $N_{173} > N_{171}+1$ the clusters either break into smaller units or evaporate. Conversely, when the unequal-spin atoms attract each other, the variability in the cluster compositions is larger, the most stable droplets being those of the type $N_p-(N_p/2-2)/(N_p/2+1, N_p/2+1)$. That can be understood as the result of having a N_p-

$(N_p/2)/(N_p/2, N_p/2)$ balanced cluster with two additional ^{171}Yb atoms located in both wings, as can be seen in the density profiles of the 28-12/(8+8) arrangement displayed in Fig. 4. The atoms in the wings are attracted by other ^{171}Yb particles with different spins and by ^{173}Yb atoms, and both attractions are what make the entire droplet stable. The reduction in the number of spin-polarized ^{173}Yb atoms decreases also the effective repulsive interaction between identical fermions, decreasing the total energy per particle. However, if we further deplete the ^{173}Yb part of the cluster, the reduction in the ^{171}Yb - ^{173}Yb interactions de-stabilize the entire structure.

ACKNOWLEDGMENTS

We acknowledge financial support from Ministerio de Ciencia e Innovación MCIN/AEI/10.13039/501100011033 (Spain) under Grant No. PID2020-113565GB-C22 and from Junta de Andalucía group PAIDI-205. We also acknowledge the use of the C3UPO computer facilities at the Universidad Pablo de Olavide.

-
- [1] F. Böttcher, J.N. Schmidt, J. Hertkorn, K. S. H. Ng, S. D. Graham, M. Guo and T. Langen, and T. Pfau, New states of matter with fine-tuned interactions: quantum droplets and dipolar supersolids, *Rep. Prog. Phys.* **84**, 012403 (2021).
- [2] Z. Luo, W. Pang, B. Liu and Y.Y. Li, and B. A. Malomed, A new form of liquid matter: quantum droplets, *Front. Phys.* **16**, 32201 (2021).
- [3] S. Mistakidis, A. Volosniev, R. Barfknecht, T. Fogarty, T. Busch, A. Foerster, P. Schmelcher, and N. Zinner, Few-body bose gases in low dimensions—a laboratory for quantum dynamics, *Physics Reports* **1042**, 1 (2023).
- [4] D. S. Petrov, Quantum Mechanical Stabilization of a Collapsing Bose-Bose Mixture, *Phys. Rev. Lett.* **115**, 155302 (2015).
- [5] C. Cabrera, L. Tanzi, J. Sanz, B. Naylor, P. Thomas and P. Cheney, and L. Tarruell, Quantum liquid droplets in a mixture of Bose-Einstein condensates, *Science* **529**, 301 (2018).
- [6] P. Cheiney, C. R. Cabrera, J. Sanz, B. Naylor, L. Tanzi, and L. Tarruell, Bright Soliton to Quantum Droplet Transition in a Mixture of Bose-Einstein Condensates, *Phys. Rev. Lett.* **120**, 135301 (2018).
- [7] G. Semeghini, G. Ferioli, L. Masi, C. Mazzinghi, L. Wolswijk, F. Minardi, M. Modugno, G. Modugno, M. Inguscio, and M. Fattori, Self-bound quantum droplets of atomic mixtures in free space, *Phys. Rev. Lett.* **120**, 235301 (2018).
- [8] I. Ferrier-Barbut, H. Kadau, M. Schmitt, M. Wenzel, and T. Pfau, Observation of quantum droplets in a strongly dipolar bose gas, *Phys. Rev. Lett.* **116**, 215301 (2016).
- [9] C. D’Errico, A. Burchianti, M. Prevedelli, L. Salasnich, F. Ancilotto, M. Modugno, F. Minardi, and C. Fort, Observation of quantum droplets in a heteronuclear bosonic mixture, *Phys. Rev. Res.* **1**, 033155 (2019).
- [10] Z. Guo, F. Jia, L. Li, Y. Ma, J. M. Hutson, X. Cui, and D. Wang, Lee-Huang-Yang effects in the ultracold mixture of ^{23}Na and ^{87}Rb with attractive interspecies interactions, *Phys. Rev. Res.* **3**, 033247 (2021).
- [11] L. Parisi and S. Giorgini, Quantum droplets in one-dimensional bose mixtures: A quantum monte carlo study, *Phys. Rev. A* **102**, 023318 (2020).
- [12] M. Tylutki, G. E. Astrakharchik, B. A. Malomed, and D. S. Petrov, Collective excitations of a one-dimensional quantum droplet, *Phys. Rev. A* **101**, 051601 (2020).
- [13] J. Wang, H. Hu, and X. Liu, Thermal destabilization of self-bound ultradilute quantum droplets, *New. J. Phys.* **22**, 103044 (2020).
- [14] L. Salasnich, S. K. Adhikari, and F. Toigo, Self-bound droplet of Bose and Fermi atoms in one dimension: Collective properties in mean-field and Tonks-Girardeau regimes, *Phys. Rev. A* **75**, 023616 (2007).
- [15] M. Tylutki, A. Recati and F. Dalfovo, and S. Stringari, Dark-bright solitons in a superfluid Bose-Fermi mixture, *New. J. Phys.* **18**, 053014 (2016).
- [16] D. Rakshit, T. Karpiuk and M. Brewczyk, and M. Gajda, Quantum Bose-Fermi droplets, *SciPost Phys.* **6**, 079 (2019).
- [17] D. Rakshit, T. Karpiuk, P. Zin, M. Brewczyk and M. Lewenstein, and M. Gajda, Self-bound Bose-Fermi liquids in lower dimensions, *New. J. Phys.* **21**, 073027 (2019).
- [18] J. C. Peacock, A. Ljepoja, and C. J. Bolech, Quantum coherent states of interacting Bose-Fermi mixtures in one

- dimension, Phys. Rev. Research **4**, L022034 (2022).
- [19] M. C. Gordillo, Self-bound clusters of one-dimensional fermionic mixtures, Phys. Rev. Res. **5**, 043144 (2023).
- [20] M. C. Gordillo, Antiferromagnetic behavior in self-bound one-dimensional composite bosons, Phys. Rev. A **109**, L061301 (2024).
- [21] J. Givois, A. Tononi, and D. S. Petrov, Self-binding of one-dimensional fermionic mixtures with zero-range interspecies attraction, SciPost Phys. **14**, 091 (2023).
- [22] G. E. Astrakharchik and S. Giorgini, Correlation functions of a Lieb-Liniger Bose gas, Journal of Physics B: Atomic, Molecular and Optical Physics **39**, L1 (2006).
- [23] D. S. Petrov, C. Salomon, and G. V. Shlyapnikov, Weakly bound dimers of fermionic atoms, Phys. Rev. Lett. **93**, 090404 (2004).
- [24] G. E. Astrakharchik, J. Boronat, J. Casulleras, and S. Giorgini, Equation of state of a Fermi gas in the BEC-BCS crossover: A quantum Monte Carlo study, Phys. Rev. Lett. **93**, 200404 (2004).
- [25] J. N. Fuchs, A. Recati, and W. Zwerger, Exactly solvable model of the BEC-BCS crossover, Phys. Rev. Lett. **93**, 090408 (2004).
- [26] M. C. Gordillo, Pairing in $SU(6) \times SU(2)$ one-dimensional fermionic clusters, Phys. Rev. A **102**, 023335 (2020).
- [27] M. Gordillo, Metal and insulator states of $SU(6) \times SU(2)$ clusters of fermions in one-dimensional optical lattices, New J. Phys. **21**, 063034 (2021).
- [28] M. Olshanii, Atomic scattering in the presence of an external confinement and a gas of impenetrable bosons, Phys. Rev. Lett. **81**, 938 (1998).
- [29] M. Kitagawa, K. Enomoto, K. Kasa, Y. Takahashi, R. Ciuryło, P. Naidon, and P. S. Julienne, Two-color photoassociation spectroscopy of ytterbium atoms and the precise determinations of s -wave scattering lengths, Phys. Rev. A **77**, 012719 (2008).
- [30] B. Hammond, W.A. Lester, and P. Reynolds, *Monte Carlo Methods in Ab Initio Quantum Chemistry* (World Scientific, Singapore, 1994).
- [31] S. Ceperley, Fermion nodes, J. Stat. Phys. **63**, 1237 (1991).
- [32] J. Carlson, S.-Y. Chang, V. R. Pandharipande, and K. E. Schmidt, Superfluid Fermi gases with large scattering length, Phys. Rev. Lett. **91**, 050401 (2003).
- [33] D. Griffiths, *Introduction to Quantum Mechanics* (Pearson Prentice Hall; 2nd edition, 2004).
- [34] E. Sola, J. Casulleras, and J. Boronat, Ground-state energy and stability limit of ^3He droplets, Phys. Rev. B **73**, 092515 (2006).
- [35] M. D. Girardeau, Tonks-Girardeau and super-Tonks-Girardeau states of a trapped one-dimensional spinor Bose gas, Phys. Rev. A **83**, 011601 (2011).
- [36] G. E. Astrakharchik, *Quantum Monte Carlo study of ultracold gases. PhD Thesis* (Università degli Studi Trento, 2004).